
Proceedings Paper:
Xiao, X orcid.org/0000-0003-0718-2591 and Wen, D orcid.org/0000-0003-3492-7982 (2018) Investigation on thermo-physical properties of molten salt enhanced with nanoparticle and copper foam. In: 2018 7th International Conference on Renewable Energy Research and Applications (ICRERA). ICRERA 2018, 14-17 Oct 2018, Paris, France. IEEE , pp. 1445-1449. ISBN 978-1-5386-5982-3

https://doi.org/10.1109/ICRERA.2018.8566907

Investigation on thermo-physical properties of molten salt enhanced with nanoparticle and copper foam

Xin Xiao[1, *]
[1]School of Chemical and Process Engineering
University of Leeds
Leeds, LS2 9JT, United Kingdom
x.xiao@leeds.ac.uk

Dongsheng Wen[1, 2]
[2]School of Aeronautic Science and Engineering
Beihang University
Beijing, 100191, China

***Abstract*—HITEC salt (40 wt.% $NaNO_2$, 7 wt.% $NaNO_3$, 53 wt.% KNO_3) with a melting temperature of about 142 °C is a typical phase change material for solar energy storage. Both aluminum oxide (Al_2O_3) nanopowder and copper foam were applied to enhance pure HITEC salt, so as to retrieve the limitation of composite PCMs with single enhancement. Nanocomposite was synthesized with two-step methods at the beginning, then copper foam were infiltrated with nano-salt at high temperature. The morphologies of the composites were extensively characterized with Scanning Electron Microscope, X-ray diffraction and Fourier Transform Infrared Spectrometer, while the thermal behaviors were analyzed with Differential Scanning Calorimeter and Thermos-gravimetric Analyser. Results showed that special nanostructures were formed in the composite, and physical bonding was found between Al_2O_3 nanopowder and salt. Theoretical prediction showed that the thermal conductivities of the composites were significantly enhanced about ten times, and the specific heat capacities of the composites were slightly decreased, which is beneficial for heat storage. Furthermore, the presence of porous copper foam and Al_2O_3 nanopowder made the extrapolated onset and peak phase change temperatures shift slightly.**

Keywords*—HITEC salt; aluminum oxide nanopowder; copper foam; structural characteristics; thermal characterization

I. INTRODUCTION

With the growing concern about the environmental issues and exhaustion of fossil fuels recently, the fuel consumption and emission regulations become strict and will be more rigorous in the future. Energy crisis promote the development of utilization of renewable energy, while energy storage especially latent heat thermal energy storage (LHTES) are combined with energy systems to overcome the time-dependant limitation. Thus solar energy as one of renewable energy always using molten salts as phase change materials (PCMs) to be the storage media are of great interest [1-4]. The low thermal conductivitity of pure salt causes the slow thermal response of the LHTES system, so it is indispensible to enhance the thermal conductivitity.

Because of its light weight and large void space, metal foams with high porosities are recommended to improve the heat transfer of PCMs [5-7]. However, they always reduce latent heat and specific heat capacity of the composite, consequently cause a less overall storage capacity. Dispersing nanoparticles into PCMs can keep and increase the specific heat capacity of the nanocomposite slightly. Ho and Pan [8] investigated the effect of nanoparticle concentrations on the heat transfer characteristics of nano-HITEC salt flowed in a circular tube. Results indicated that the precipitation phenomenon can be retrieved using the innovative apparatus. Both the mean and local Nusselt number exhibited significant enhancement with the addition of aluminum oxide (Al_2O_3) nanopowder. Liu and Yang [9] investigated the specific heat capacity and latent heat of $Na_2CO_3{\cdot}10H_2O$-$Na_2HPO_4{\cdot}12H_2O$ doped with TiO_2 nanoparticles. They pointed out that the specific heat capacities increased by 83.5% in solid state and 15.1% in liquid state with the addition of 0.3% TiO_2. Song et al. [10] experimentally investigated the effects of the mixing time and stirring rate of preparation of molten-salt nanofluids on the specific heat capacity of quaternary nitrate dispersed with SiO_2 nanoparticles. It was found that the specific heat capacity of the molten-salt nanofluids could be enhanced due to the formation of nanostructures, while the similar phenomenon was also reported in the research of Huang et al. [11]. It can be seen that it is of great importance to incorporate of high-conductive nanoparticles into metal foam, so as to make the attractive enhancement of pure PCMs.

In the present study, HITEC salt (40 wt.% $NaNO_2$, 7 wt.% $NaNO_3$, 53 wt.% KNO_3) as a typical molten salt was used as the base PCM. Al_2O_3 nanopowder with the mass fraction of 3.0% and copper foam with the porosity of 95.0% were added into salt, Al_2O_3 nanopowder seeded HITEC salt/copper foam composite were prepared and characterized subsequently. The morphologies of the composites were extensively characterized with Scanning Electron Microscope (SEM), X-ray diffraction (XRD) and Fourier Transform Infrared Spectrometer (FT-IS), while the thermal behaviors were analyzed with Differential Scanning Calorimeter (DSC) and Thermos-gravimetric Analyser (TGA).

II. CHARACTERIZATION METHODS

A. Preparation of composite PCMs

Sodium nitrite, sodium nitrate, and potassium nitrate were uniformly mixed with the mass ratios of 40:7:53, and Al_2O_3 nanopowder and copper foam were used to enhance the thermo-physical properties of pure salt. Firstly, HITEC

salt/Al_2O_3 nanocomposite was made with two-step methods (Fig. 1). Pure salt was dissolved into deionized water, and Al_2O_3 nanopowder with the mass fraction of 1%, 2% or 3% was dissolved in the suspension, respectively, which was sonicated 1 h for good dispersion. Then copper foam with the porosity of about 95.0% was physically immersed in the solution. Finally the solution with sonication was reheated in an oven at 200 °C to evaporate the water and make good impregnation. Then the porous copper foam impregnated with salt/Al_2O_3 nanocomposite was taken out, as shown in Fig. 1.

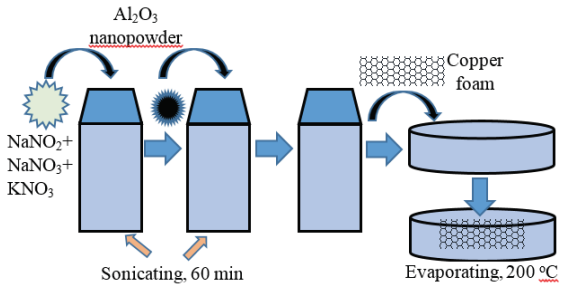

Fig. 1. Synthesis of Al_2O_3 nanopowder seeded salt/copper foam composite.

B. Morphologies of the nanoparticle-seeded salt

Series characterization of thermo-physical properties of the composites were addressed subsequently. The morphologies of the composites were characterized by tabletop Microscope TM3030 as the SEM. XRD Bruker D8 with a vantec detector and FTir - Thermo iS10 were used as the suppliment of the component analysis, so as to analyze the chemical bonding, molecular structure and degradation effect of the specimens. The specimens were scanned by X-rays with the rotated angle from 10° to 60°. When FT-IR was used, infrared was transmitted through the specimens and the absorption and emission of wave length from the specimen were monitored, and FT-IR Perkin Elmer device covers wavelength ranged from 400 cm^{-1} to 4000 cm^{-1}.

C. Thermal characterization of the composite PCMs

Al_2O_3 nanopowder used in the present study are with the density of 3900.0 kg/m^3 and thermal conductivity of 46.0 W/(m K) [12]. The volume fraction (Φ) of Al_2O_3 nanopowder is about 0.53%, 1.07% or 1.61% when the mass fraction is 1%, 2% or 3%, respectively. Then the effective thermal conductivities (λ) of the salt/copper foam composite seeded with Al_2O_3 nanopowder were theoretically predicted with the literature models. The modified Maxwell-Garnett models [13] including Brownian motion and nanoparticles aggregation was used to estimate the thermal conductivity of nanocomposite, as shown in (1).

$$\frac{\lambda_{nc}}{\lambda_{PCM}}=\frac{\lambda_{np}+2\lambda_{PCM}-2\Phi\left(\lambda_{PCM}-\lambda_{np}\right)}{\lambda_{np}+2\lambda_{PCM}+\Phi\left(\lambda_{PCM}-\lambda_{np}\right)}+\frac{\rho_{np}\Phi c_{p\text{-}np}}{2\lambda_{PCM}}\sqrt{\frac{2K_BT}{3\pi d_{np}\mu_{PCM}}} \quad (1)$$

The structural models were used to predict the effective thermal conductivity of the composite fabricated by porous medium. The model combined the series and parallel models together and another model constructed of unit cell with hexagonal structure were both used in the present study, as shown in (2)-(5) [14].

$$\lambda_{eff}=\left(\varepsilon\lambda_{nc}+\left(1\text{-}\varepsilon\right)\lambda_{sk}\right)^{F}\left(\frac{1}{\left(\frac{\varepsilon}{\lambda_{nc}}+\frac{1-\varepsilon}{\lambda_{sk}}\right)}\right)^{1-F} \quad (2)$$

where the parameter F is calculated as follows:

$$F=1.0647\left(0.3031+0.0623\ln\left(\varepsilon\frac{\lambda_{sk}}{\lambda_{nc}}\right)\right) \quad (3)$$

The unit cell model is as follows:

$$\lambda_{eff}=\left(\left(\frac{2}{\sqrt{3}}\right)\left(\frac{r\left(\frac{b}{L}\right)}{\lambda_{nc}+\left(1+\frac{b}{L}\right)\frac{\left(\lambda_{sk}-\lambda_{nc}\right)}{3}}+\frac{\left(1-r\right)\left(\frac{b}{L}\right)}{\lambda_{nc}+\frac{2}{3}\left(\frac{b}{L}\right)\left(\lambda_{sk}-\lambda_{nc}\right)}+\frac{\frac{\sqrt{3}}{2}-\frac{b}{L}}{\lambda_{nc}+\frac{4r}{3\sqrt{3}}\left(\frac{b}{L}\right)\left(\lambda_{sk}-\lambda_{nc}\right)}\right)\right)^{-1} \quad (4)$$

$$\frac{b}{L}=\frac{-r+\sqrt{r^2+\frac{2}{\sqrt{3}}\left(1-\varepsilon\right)\left(2-r\left(1+\frac{4}{\sqrt{3}}\right)\right)}}{\frac{2}{3}\left(2-r\left(1+\frac{4}{\sqrt{3}}\right)\right)} \quad (5)$$

where r is the area ratio and equals to 0.09, and b/L is the dimensionless parameter of length ratio.

Mettler-Toledo DSC was used to characterize the phase change behaviour of the composites. All the specimens were slightly heated until they reached 50 °C firstly. Then they were subjected to melting–freezing cycles under the same test conditions with the heating and cooling rates of 5 °C /min and temperature range of 50~200 °C. Two thermal cycles were conducted and the average values were used to characterize the peak temperatures and extrapolated onset temperatures. In addition, the specific heat capacities were measured and calculated with the multiple methods. Mettler-Toledo TGA was used to detect the variation of weight reduction when the specimens were heated from 40 °C to 850 °C. Nitrogen (99.999%) was used as carrier with a flow rate of 50 mL/min by following the ASTM E-1131 method.

III. Results and Discussion

A. Characterization of composite PCMs

Fig. 2 shows the SEM images of salt/Al_2O_3 nanocomposite with and without copper foam. It can be seen that the salt/Al_2O_3

nanocomposite is totally compatible with copper foam. The rugged surface in Fig. 2 (b) was caused by the shrinkage of salt during freezing. Fig. 2 (d) shows that Al_2O_3 nanopowder can mix well with salt, and the nanopowder can generate chemical structure interaction with salt molecules.

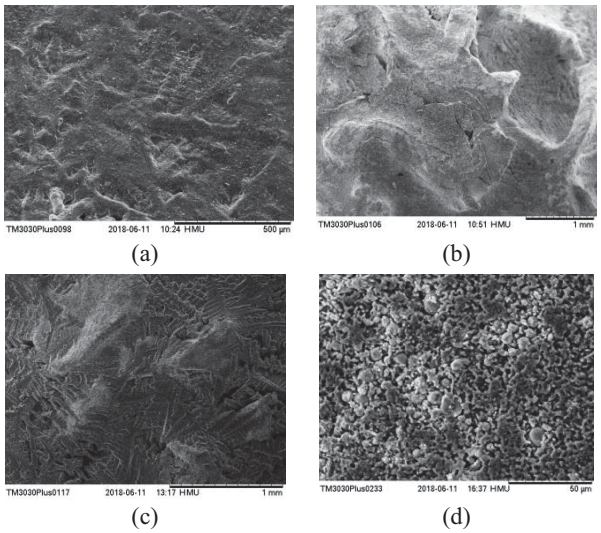

Fig. 2. SEM images of HITEC salt/copper foam composite seeded with Al_2O_3 nanopowder, 1 wt.% Al_2O_3 nanopowder (a) 2 wt.% Al_2O_3 nanopowder (b) 3 wt.% Al_2O_3 nanopowder (c) and 3 wt.% Al_2O_3 nanopowder without copper foam (d).

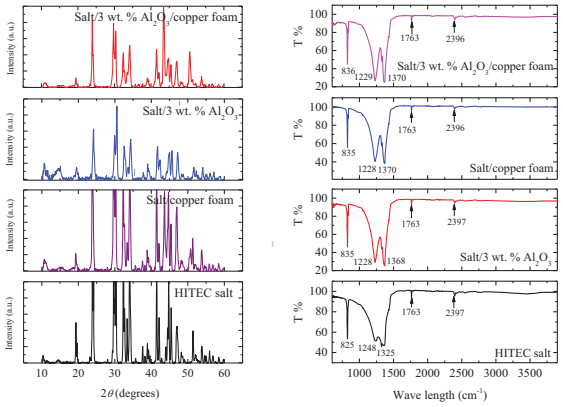

Fig. 3. XRD and FT-IR analyses of HITEC salt and composite PCMs

Fig. 3 shows the XRD and FT-IR analyses of HITEC salt and salt/copper foam composite seeded with Al_2O_3 nanopowder. The results obtained from the XRD analysis show that pure salt and all composite PCMs have no obvious changes of intensity peaks. Some peaks seem sharply increase with the addition of copper foam, while the peaks slightly decrease with the addition of Al_2O_3 nanopowder. The reason is that the physical bonding of Al_2O_3 nanopowder with nitrate molecule was formed during the synthesis process.

FT-IR analysis of the specimens are also shown in Fig. 3. It can be seen that the FT-IR absorption spectra are nearly the same for all the specimens, indicating that the existence of the physical bonding of Al_2O_3 nanopowder with nitrate molecule does not disturb the chemical structure interaction for chemical stability. The peaks between 1200 cm^{-1}~1400 cm^{-1} are slightly apparent with the addition of Al_2O_3 nanopowder and copper foam, indicating that the good bonding between Al_2O_3 nanopowder and nitrate molecule exists.

B. Effective thermal conductivities of composite PCMs

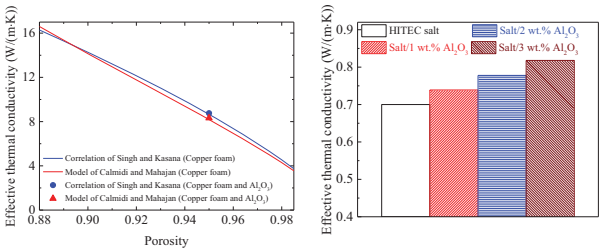

Fig. 4. Effective thermal conductivities of HITEC salt and composite PCMs

Fig. 4 shows the prediction of the effective thermal conductivities of the composites. The effective thermal conductivities of the salt/Al_2O_3 nanocomposite are 0.739 W/(m K), 0.778 W/(m K), 0.818 W/(m K) with the addition of 1 wt.%, 2 wt.% and 3 wt.% Al_2O_3 nanopowder, respectively. While the thermal conductivity of the salt/copper foam composite seeded with 3 wt.% Al_2O_3 nanopowder can reach 8.32 W/(m K) using the Calmidi and Mahajan model, comparing with pure salt of about 0.7 W/(m K), as shown in Fig. 4(a).

C. Thermal behaviour of composite PCMs

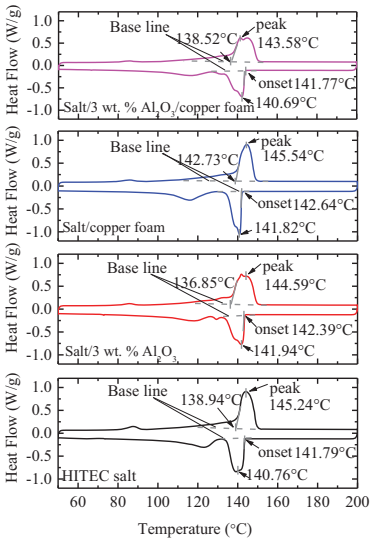

Fig. 5. DSC curves of HITEC salt and composite PCMs

The variations of the phase change temperatures of salt/copper foam seeded with Al_2O_3 nanopowder were characterized with DSC, as shown in Fig. 5. The extrapolated onset melting temperature of the salt/3 wt.% Al_2O_3 nanocomposite shifts from 138.94 ºC to 136.85 ºC, while the extrapolated onset freezing temperature shifts from 141.79 ºC to 142.39 ºC, compared with those of pure salt. The addition of Al_2O_3 nanopowder can slightly decrease the extrapolated onset melting temperature and increase the extrapolated onset freezing temperature of pure salt, that is, it can promotes the early occurrence of phase change onset temperature. The phenomenon can be attributed to the good combination and dispersion performance of the PCM and promoter. On the contrary, the extrapolated onset and peak melting temperatures of the salt/copper foam composite display different characteristics from the salt/Al_2O_3 nanocomposite, shifting slightly to higher temperatures. The deviated tendency of the melting temperatures can be explained by the Clapeyron-Clausius equation, and the same phenomenon has been reported in the previous study [15]:

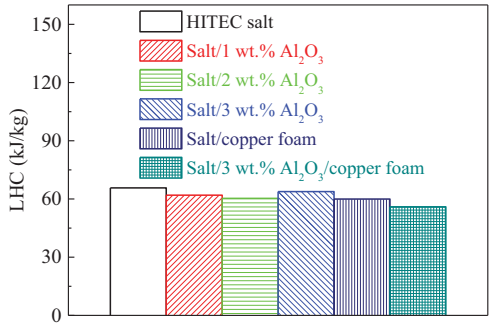

Fig. 6. Latent heat of HITEC salt and composite PCMs

The LHC (latent heat per mass composite) of HITEC salt and composite PCMs obtained by numerical integration of the area under the heat flow curves are shown in Fig. 6. It can be seen that the LHC of the composite PCMs is lower than that of HITEC salt as Al_2O_3 nanopowder and copper foam cannot take part in the phase change process. However, the decrease of the LHC of the composite PCMs was not accurately proportional to the mass fraction of the added Al_2O_3 nanopowder or copper foam. The LHC of the salt/3 wt.% Al_2O_3 nanocomposite is 63.79 kJ/kg, while that of the salt/copper foam composite PCM is 59.96 kJ/kg, indicating that Al_2O_3 nanopowder can slightly increase the LHC because of the formation of nanostructure inside the composite.

Table 1 lists the specific heat capacities of HITEC salt and composite PCMs. It shows that the specific heat capacities of the nanocomposites are apparently enhanced with the addition of Al_2O_3 both in solid and liquid states, while those of the salt/copper foam composite PCMs decrease, compared with that of pure salt. The maximum enhancement is about 12.1% in solid state, and about 5.8% in liquid state with a nanoparticle concentration of 2.0 wt.%, which was due to the increase of molecular energy [16].

TABLE I. SPECIFIC HEAT CAPACITY OF HITEC SALT AND COMPOSITE PCMS

Specific heat capacity (kJ/kg·ºC)	HITEC salt	+Al_2O_3			HITEC salt/copper foam	HITEC salt/copper foam/3 wt.% Al_2O_3
		1 wt.%	2 wt.%	3 wt.%		
Solid state	1.40	1.57	1.57	1.54	1.32	1.42
Liquid state	1.56	1.65	1.65	1.62	1.50	1.51

D. Thermogravimetric analysis of composite PCMs

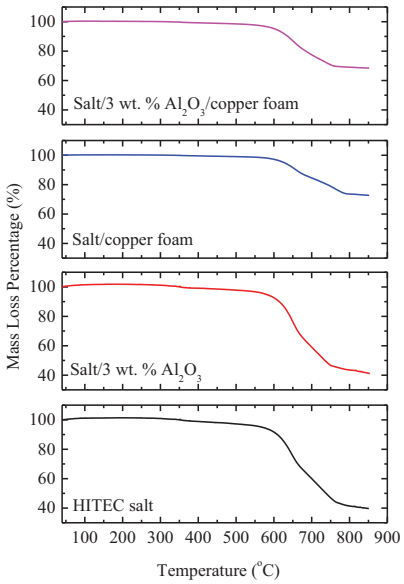

Fig. 7. Thermo-gravimetric analysis of HITEC salt and composite PCMs

Fig. 7 shows the TGA curves of HITEC salt and composite PCMs. HITEC salt is stable up to about 550 ºC, then rapid degradation of the salt happens. It can be seen that nearly 60% of the mass loses between 550°C and 800°C. A solid stable compound may be produced as the weight slightly changes above 800°C. The solid mass left in the crucible will probably be a blend of potassium and sodium oxide. In addition, the composite PCMs with copper foam shows larger mass left as the metal skeleton can be kept over 800 ºC.

IV. CONCLUSIONS

In the present study, HITEC salt was used as the base PCM, and Al_2O_3 nanopowder and copper foam were combined to enhance the salt. The composite PCMs were synethesised and characterized, and the following conclusions can be drawn:

(1) SEM image indicates that pure salt can mix well with Al_2O_3 nanopowder using the two-step methods. Morphology investigation shows that the salt/Al_2O_3 nanocomposite is totally compatible with copper foam, and no obvious changes of wavelength peaks are found with FT-IR analysis.

(2) The effective thermal conductivity of the salt/copper foam composite seeded with 3 wt.% Al_2O_3 nanopowder can increase by ten times and reach about 8.32 W/(m K), compared to that of pure salt of 0.7 W/(m K).

(3) The extrapolated onset and peak melting and freezing temperatures of the composites shift slightly, compared with those of pure salt, e.g. the extrapolated onset melting temperature of the salt/3 wt.% Al_2O_3 nanocomposite shifts from 138.94 ºC to 136.85 ºC, while the extrapolated onset freezing temperature shifts from 141.79 ºC to 142.39 ºC.

(4) The specific heat capacity of HITEC salt/copper foam composite seeded with Al_2O_3 nanopowder is reduced by about 3.2% in liquid state, while that of the salt/2 wt.% Al_2O_3 nanocomposite increases about 5.8%, compared to that of pure salt.

ACKNOWLEDGMENT

X. Xiao thanks European Union's Horizon 2020 research and innovation programme under the Marie Sklodowska-Curie grant agreement (No.706788).

REFERENCES

[1] A. Bonk, S. Sau, N. Uranga, M. Hernaiz, and T. Bauer, "Advanced heat transfer fluids for direct molten salt line-focusing CSP plants," Prog. Energ. Combust., vol. 67, pp. 69-87, 2018.

[2] M.A. Taher and M.N. Fares, "Experimental investigation of solar energy storage using paraffin wax as thermal mass," Int. J. Renew. Energy Res., vol. 7, pp. 1850-1856, 2017.

[3] B.M. Goortani and H. Heidari, "Advanced modeling of CSP plants with sensible heat storage: Instantaneous effects of solar irradiance," Int. J. Renew. Energy Res., vol. 7, pp. 1419-1425, 2017.

[4] M. Chiandone, C. Tam, R. Campaner, and G. Sulligoi, "Electrical storage in distribution grids with renewable energy sources," in Proc. of 2017 International Conference on Renewable Energy Research and Applications (ICRERA), 2017.

[5] M. Nazari, M. Ashouri, M.H. Kayhani, and A. Tamayol, "Experimental study of convective heat transfer of a nanofluid through a pipe filled with metal foam," Int. J. Therm. Sci., vol. 88, pp. 33-39, 2015.

[6] J.M. Mahdi and E.C. Nsofor, "Solidification enhancement in a triplex-tube latent heat energy storage system using nanoparticles-metal foam combination," Energy, vol. 126, pp. 501-512, 2017.

[7] Q.L. Ren, F.L. Meng, and P.H. Guo, "A comparative study of PCM melting process in a heat pipe-assisted LHTES unit enhanced with nanoparticles and metal foams by immersed boundary-lattice Boltzmann method at pore-scale," Int. J. Heat Mass Tran., vol. 121, pp. 1214-1228, 2018.

[8] M.X. Ho and C. Pan, "Experimental investigation of heat transfer performance of molten HITEC salt flow with alumina nanoparticles," Int. J. Heat Mass Tran., vol. 107, pp. 1094-1103, 2017.

[9] Y.S. Liu and Y.Z Yang, "Investigation of specific heat and latent heat enhancement in hydrate salt based TiO_2 nanofluid phase change material," Appl. Therm. Eng., vol. 124, pp. 533-538, 2017.

[10] W.L. Song, Y.W. Lu, Y.T. Wu, and C.F. Ma, "Effect of SiO_2 nanoparticles on specific heat capacity of low-melting-point eutectic quaternary nitrate salt," Sol. Energy Mat. Sol. C., vol. 179, pp. 66-71, 2018.

[11] Y. Huang, X.M. Cheng, Y.Y. Li, G.M. Yu, K. Xu, and Ge Li, "Effect of in-situ synthesized nano-MgO on thermal properties of $NaNO_3$-KNO_3," Sol. Energy, vol. 160, pp. 208-215, 2018.

[12] K.C. Lin and A. Violi, "Natural convection heat transfer of nanofluids in a vertical cavity: Effects of non-uniform particle diameter and temperature on thermal conductivity," Int. J. Heat Fluid Flow, vol. 31, pp. 236-245, 2010.

[13] Y.M. Xuan, Q. Li, and W.F. Hu, "Aggregation structure and thermal conductivity of nanofluids,"AIChE J, vol.49, pp. 1039-1043, 2003.

[14] X. Xiao, P. Zhang, and M. Li, "Effective thermal conductivity of open-cell metal foams impregnated with pure paraffin for latent heat storage," Int. J Therm. Sci., vol. 81, pp. 94-105, 2014.

[15] X. Xiao, P. Zhang, and M. Li, "Preparation and thermal characterization of paraffin/metal foam composite phase change material," Appl. Energy, vol. 112, pp. 1357-1366, 2013.

[16] Y.W. Hu, Y.R. He, Z.D. Zhang, and D.S. Wen, "Effect of Al_2O_3 nanoparticle dispersion on the specific heat capacity of a eutectic binary nitrate salt for solar power applications," Energy Convers. Manage., vol. 142, pp. 366-373, 2017.